해부 · 생물인류학 제 35 권 제 2 호
Anat Biol Anthropol Vol. 35, No. 2 (2022) pp. 57~66
https://doi.org/10.11637/aba.2022.35.2.57

Check for updates

Original Article

Deep Tissue Clearing for Three-dimensional Imaging Analysis of Murine Pancreas

Nanda Maya Mali[1,2,†], Jung Min Park[1,3,†], Gil-Hyun Kim[4], Dong-Hwa Choi[5,6], Raul Ramos[7], Jong Hyuk Lee[8], Eu Jeong Ku[9,10], Ji Won Oh[1,2,3,11,12]

[1]*Department of Anatomy, Kyungpook National University, School of Medicine*
[2]*Bio-Medical Research Institute, Kyungpook National University Hospital*
[3]*Immune Square Inc.*
[4]*Binaree, Inc.*
[5]*Biocenter, Gyeonggido Business & Science Accelerator*
[6]*Graduate School of East-West Medical Science, Kyung Hee University*
[7]*Department of Developmental and Cell Biology, University of California, Irvine*
[8]*Department of Artificial Intelligence & Big Data Engineering, Daegu Catholic University*
[9]*Department of Internal Medicine, Chungbuk National University Hospital*
[10]*Department of Internal Medicine, Chungbuk National University, College of Medicine*
[11]*Clinical Omics Institute, Kyungpook National University*
[12]*Department of Anatomy, Yonsei University College of Medicine*

Abstract : Optical imaging of the vascular system is necessary for structural, functional, developmental, and pathological biology. Recent developments in optical tissue-clearing methods have significantly advanced large-scale tissue researches by integrating a three-dimensional (3D) visualization of topographical vasculature, so we aimed to enhance the vascular structure of the murine pancreas which are highly vascularized structure. In this study, the adult C57/BL6 murine pancreatic tissue was cleared after lectin staining, resulting in the reconstructed structures for 3D imaging within a short period without damaging. Enhancing the visualization processes using light-sheet fluorescence microscopy (LSFM) together with 3D reconstruction imaging tool, we studied in depth of the entire vascular system, which further enabled to reconstruct 3D structure of the vasculature in pancreas and islets. We successfully implemented the normal murine pancreatic tissues including exocrine and endocrine

[†]These authors contributed equally to this work.

This work was supported by the research grant of the Chungbuk National University Hospital in 2021 (Dr. Eu Jeong Ku). The funding source did not have any input in the study design, data collection, interpretation of the results, preparation of the manuscript, or publishing decision.
The author(s) agree to abide by the good publication practice guideline for medical journals.
The author(s) declare that there are no conflicts of interest.
Received: April 14, 2022; **Revised:** May 26, 2022; **Accepted:** May 26, 2022
Correspondence to: Ji Won Oh (Department of Anatomy, Yonsei University College of Medicine, 50-1, Yonsei-ro Seodaemun-gu, Seoul, Korea)
Eu Jeong Ku (Department of Internal Medicine, Chungbuk National University Hospital, Chungbuk National University College of Medicine, 776, 1Sunhwan-ro, Seowon-gu, Cheongju, 28644, Korea)
E-mail: g1@yuhs.ac.kr, eujeong.ku@gmail.com

www.kci.go.kr
© 2022 Korean Association of Physical Anthropologists
This is an Open Access article distributed under the terms of the Creative Commons Attribution Non-Commercial License (http://creativecommons.org/ licenses/by-nc/3.0) which permits unrestricted non-commercial use, distribution, and reproduction in any medium, provided the original work is properly cited.
ISSN 2671-566X (Online) · ISSN 2671-5651 (Print)

cells and vascular structures, reflecting pancreatic β-cell function. The size of islets of each pancreatic lobe were not different but the number of islets in each lobe was variable in our quantification. In conclusion, this deep tissue clearing technique for 3D imaging could be applied in future studies to further understand the topological interactions of various cells and blood vessels within intact organs and tissues.

Keywords : Light-sheet fluorescence microscopy, Pancreas, Three-dimensional, Tissue clearing, Vascular system

INTRODUCTION

Three-dimensional (3D) visualization analyses allows for the investigation of anatomical and cellular interactions that are not easily understood from typical two-dimensional (2D) histological analyses [1,2]. To overcome several limitations including time-consuming and error-prone procedure of conventional 3D image reconstruction, various optical tissue-clearing methods have been developed to render opaque tissues transparent [3-5].

Generally, tissues are presented in an opaque state in response to light scattering and varying refractive index values of tissue components, so tissues can be cleared either by removing the light scattering element or adding a reagent that matches the average refractive index of the specific tissue components [6]. This highlights the importance of selecting the proper tissue clearing method to not only conserve experimental resources but also provide reliable and reproducible results. It is also necessary to use appropriate imaging methods that provide high resolution with decent macroscopic depths within transparent tissue. For this purpose, the use of light-sheet fluorescence microscopy (LSFM) is increasingly becoming accepted as the most appropriate method and accompanying tool to achieve high-resolution results. The LSFM has specialized lasers designed to penetrate deeper into tissues, providing multiple precise optical-section imaging together with high-speed capture of large tissues. The imaging of large volume tissues under the LSFM with a sheet of light allows the tissue specimen to be clearer, making it easier to show cellular diversity in the entire tissue. Further, the microscope provides high signal-to-noise ratio with minimum photobleaching [7].

The topological structure of the vascular system is highly linked to its functions [8]. Functional aspects in which the branching pattern and spatial distribution of blood vessels have an important influence can be examined through 3D imaging. In addition to deep tissue imaging, organoids and spheroids can also benefit from tissue clearing to visualize spatiotemporal interactions between cells [9]. Alteration of glucose homeostasis is regarded as the definition of diabetes, pathological investigations of the pancreas are mainly focused on changes in the islets of Langerhans. Early complete β-cell loss is observed in autoimmune-mediated or fulminant type 1 diabetes, whereas β-cell mass is known to decrease by 30%∼50% in type 2 diabetes [10]. In this regard, identifying information about the volume and structure of the pancreas is potentially a significant indicator for both prognoses and clinical management of diabetic patients. Recent advances in pancreatic imaging technology using computed tomography (CT) or magnetic resonance imaging (MRI) allow the size or volume of the pancreas to be measured with relatively high precision. However, determining pathophysiological conditions and predictions reflecting pancreatic function is still challenging [11,12]. The vascular structure and functioning of the pancreas are highly interlinked; this is because insulin regulates blood glucose, secreted by β-cells of islets directly into pancreatic blood vessels [13]. Many of the arteries, arterioles, and capillaries constitute the microvasculature system of the pancreas [14]. Islets are highly vascularized structures, with each islet containing 1∼5 arterioles further divided into capillaries, which forms a 5∼10 times denser capillary network than of that in exocrine pancreatic cells [15]. Today, however, methods for comprehensive 3D imaging of pancreatic vasculature remain largely unexplored.

The tissue clearing and 3D imaging is the indispensable for cellular profiling and spatiotemporal studies in the entire tissue. The major goal of this study is to show the topological structure of the vascular systems in the intact organ and study how these vessels interact with each other in the biological system, resolving the current limitation of a traditional 2D imaging. In this study, it was hypothesized that

www.kci.go.kr

a 3D visualization of the pancreatic vascular system could elucidate stereo-topological interactions within intact tissue. The present report details protocols for high-resolution imaging of the vascular system by using LSFM. Further, the study also demonstrates how to apply 3D imaging for the functional morphological assessment of pancreatic tissues by providing comprehensive reconstructed videos from different angles.

MATERIALS AND METHODS

1. In vivo perfusion and blood vessel staining

All the animal study was conducted according to the guidelines of the Committee on Animal Resources and approved by Kyungpook National University Institutional Review Board (approved number 2020 0096). Adult C57/BL6 mice (n=3) were anesthetized using a rodent inhalation anesthesia apparatus (VetEquip Inc., CA, USA), which was equipped with vaporizers issuing isoflurane (Hana Pharm Inc., Seoul, Korea). To serve as a carrier gas, 100% oxygen was used at a flow rate of 400 mL/min. For blood vessel staining, the mice were injected with 100 μL *Lycopersicon Esculentum* Lectin (2 mg conjugate/mL LEL; BioActs, Incheon, Korea), a bright-red tomato LEL-fluorophore conjugate widely used for marking blood vessels. A 25-g butterfly needle (Beckon Dickinson, NJ, USA) was inserted into the left ventricle of the mouse heart. The mice were then inserted with ~30 mL 1X phosphate-buffered saline (PBS, Biosesang, Seongnam, Korea) at pH 7.4 through the left ventricle access for 5 min or till the color of liver converts into pale. A small incision was made into the right atrium in order to drain blood. Then, a fixative solution of 4% paraformaldehyde (Biosesang, Seongnam, Korea) was inserted through the left ventricle for 20 min. The whole perfusion method was performed with a MINIPULS 3 peristaltic pump (Gilson Inc., Middleton, USA) with flow rate 7 mL/min. After perfusion, the pancreas was extracted and immersed in 4% paraformaldehyde for 12 h. The experimental workflow is illustrated in Fig. 1A.

2. Tissue clearing

The whole pancreatic tissue was cleared by using the Binaree Tissue Clearing Starter Kit (Cat. HRTC 101, Binaree, Daegu, Korea). For this process, the fixed intact pancreas tissues were immersed in a starting fixing solution at 4°C for 24 h, and then incubated with the tissue-clearing solution in a shaking incubator at 50 rpm at 37°C for 48 h. The whole intact tissue was relatively larger so the clearing step was repeated for optimum tissue clarity. After three rinses in the washing solution, the tissues were incubated in a mounting and storage solution at 25°C for 24 h. Then, imaging of cleared tissue samples was performed using the LSFM with mounting and storage solution (Cat. HRTC 101-3, Binaree, Daegu, Korea).

3. Imaging with light-sheet fluorescence microscopy and analysis

The blood vessel structure of the pancreas was imaged using a Light-sheet Z.1 Fluorescence Microscope with 5×/0.1 dual-sided illumination optics and a Plan-Neofluar 5×/0.16 objective lens (Zeiss Corporation, Jena, Germany). Fluorescence was excited with 488 nm and 561 nm wavelength lasers. Emission was detected using 505~545 nm and 575~615 nm band-pass filters. All imaging data from LSFM was saved into a CZI file using ZEN software (Zeiss). Images were reconstructed and 3D-rendered using Imaris software (Bitplane, Zurich, Switzerland). To create a 3D-constructed image of the pancreatic vascular system, thousands of Z-section images were collected through using light-sheet microscopy. All images were serially traced, stacked, and reconstructed into a 3D structure of the pancreas. Whole LSFM images and image rendering data were acquired in the Brain Research Core Facility (BRCF) of the Korea Brain Research Institute, Daegu, Korea.

4. Histological staining in 2D slides

Total three mice were used for the histological analysis. Paraffin-embedded tissues were sectioned at a thickness of ~5 μm. Before staining, tissue slides were deparaffinized with xylene (Junsei, Tokyo, Japan) and rehydrated using graded alcohol concentrations as previously described [16,17]. Lectin staining was performed according to previous described with brief modifications [18]. Briefly, rehydrated paraffin-embedded tissue slides were washed in 1X PBS for 5 min. Slides were blocked by 3% Bovine Serum Albumin (BSA, Sigma, St. Louis, USA) and then incubated with FSD™ 488 LEL lectin (BioActs, Incheon, Korea) at a 1 : 500 dilution set at room temperature for 2 h in the dark. The tissue slides were then washed in 1X PBS

www.kci.go.kr

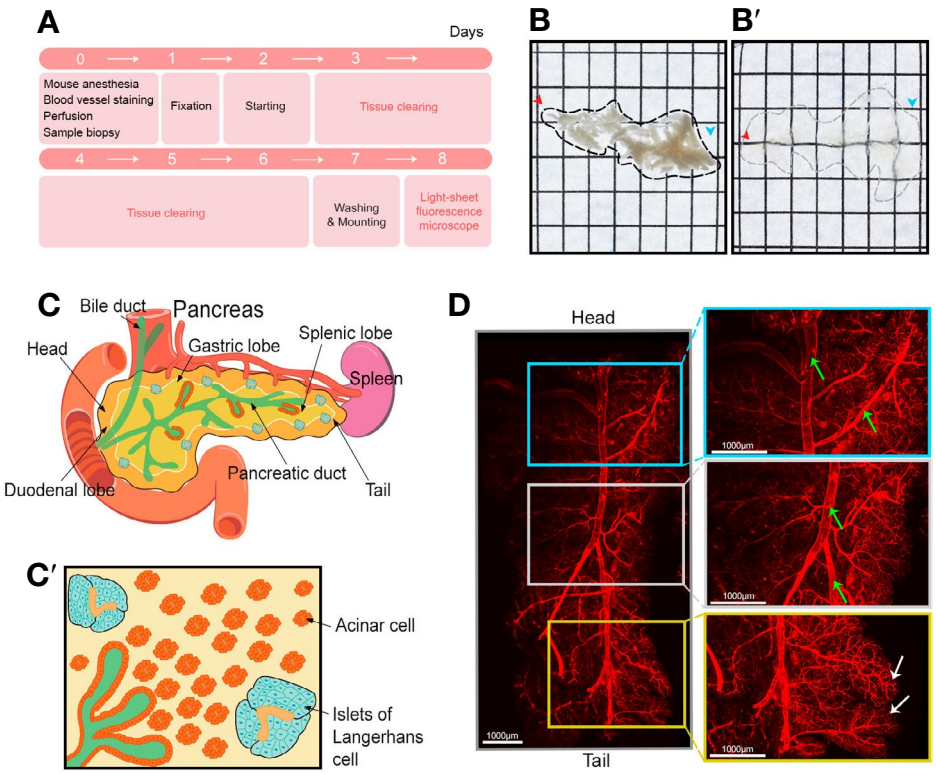

Fig. 1. The experimental workflow of tissue clearing and 3D reconstruction of the pancreas. (A): General experimental procedure and timeline for tissue clearing and imaging. Cardiac perfusion was performed after blood-vessel staining on day 1. The pancreas was cleared on day 6 and day 8; vascular images were captured and evaluated under a light-sheet fluorescence microscope. (B): Optical imaging of pancreas before (B) and after (B′) performing tissue clearing. (C): Graphical representation of an intact murine pancreas. It can be divided into two parts, the head and tail. The head part is attached with a duodenum, whereas the tail part is attached to the spleen. Three lobes of a murine pancreas were studied along with their respective organs. (C′): Exocrine and endocrine cells of the pancreas. Irregular endocrine islet cells were surrounded by exocrine acinar cells. (D): General vascular structure of the pancreas, including both major and minor blood vessels; the vessels are shown with different colored arrows: major vessels (green arrow) and minor blood capillaries (white arrow). Scale: (D): 1,000 μm.

and mounted in a DAPI-containing mounting solution (Vector Laboratories, CA, USA). Slides were imaged with a fluorescence microscope (Olympus, Tokyo, Japan). Similarly, paraffin-embedded tissue sections were stained by the combined method of hematoxylin (abcam, Cambridge, UK) and eosin (Daejung chemical and metals Co. Ltd, Siheung, Korea) (H&E) after rehydration, as previously described [16]. Stained tissue sections were imaged by using light microscope (Olympus, Tokyo, Japan).

5. Quantifying the volume of islets

The entire vessel network volume in islet cells was determined by using Imaris, as previously described [19]. To quantify the size of islets, Z-stack images were opened in Imaris and gathered automatically into a multichannel 3D model. A surface tool was used to generate the region of location in the area of interest (ROI). After reorganization of ROI, the average volume of the specific area was analyzed. This measurement was rounded down to the nearest whole number and entered as "diameter of the largest sphere that fits the object" in the surface creation wizard. The volume of each islet in duodenal lobe, gastric lobe and splenic lobe were analyzed using *t*-test for each lobe comparison and ANOVA for the group of every lobe.

RESULTS

1. Tissue clearing and blood vessels in a murine pancreas

As shown in Fig. 1A, the timeline of an experiment from sacrifice to reconstruction of images was 8 days on average.

www.kci.go.kr

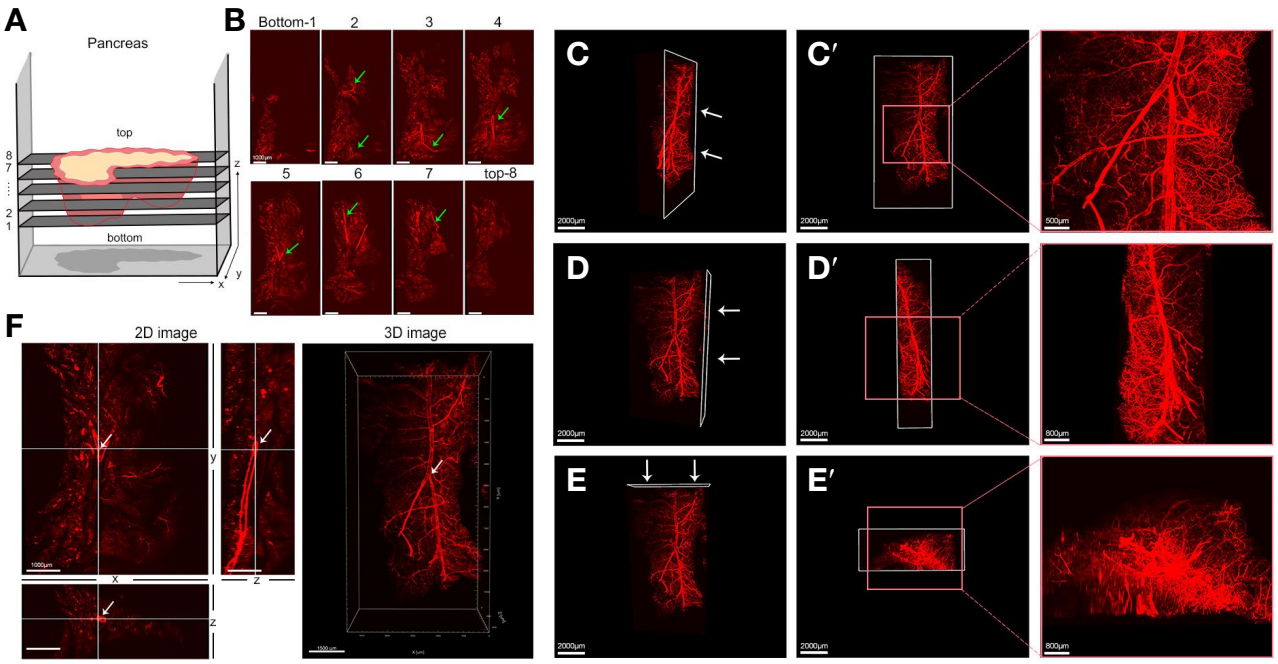

Fig. 2. 3D structure of pancreas vessel networks. (A): 3D imaging strategies and image acquisition of pancreas blood vessels. (B): Tissue imaged along the z-axis for 3D image reconstruction of an organ, conducted by stacking all available images. For example, eight images of the pancreas were taken at a specific angle to reconstruct the 3D pancreas structure; images were taken from the (1) to the top (8). (C∼E′): Optically clear pancreas imaged by the light-sheet microscope to show the vascular system. Virtual vertical (C∼D′) and horizontal (E, E′) planes of the pancreas used for 3D reconstruction. Magnified portions of pancreatic vessels are indicated by pink squares. (F): Reconstruction of 2D to 3D image. The arrow indicated a same point showing in different planes (x-y axis, y-z axis and x-z axis in 2D). Scale: (B): 1,000 μm, (C∼E'): 2,000 μm, (F): 1,000 μm, 1,500 μm.

Using the tissue clearing solution, the pancreatic tissue was sufficiently cleared to visualize the blood vessel without physically sectioning the vessel (Fig. 1B, B′). The murine pancreas is locally dispersed within the mesentery, adjacent to the small intestine, and is differentiated into three separate lobes: duodenal, splenic, and gastric (Fig. 1C, C′).

The major blood vessels, including pancreatic vessel, are shown in Fig. 1D (upper panel) as well as Supplementary Data Video 1. The capillary network is visualized through the optically-cleared tissue shown in Fig. 1D (down panel and Supplementary Data Video 2).

2. Blood vessel imaging procedure

Transparent pancreatic tissue was used for LSFM imaging (Fig. 2A∼F). The pancreatic vasculature structure was 3D-constructed (x, y, and z-axis). The horizontal plane (z-axis) was used for imaging (Fig. 2A). Several shots were taken from bottom to top surface of tissue (Fig. 2B). For 3D structuring, approximately 246 shots of 2D tissue images with approximately 2,200 μm depth of pancreas tissue were acquired in this study. The virtual horizontal and vertical planes of the 3D-reconstruted pancreatic blood vessels were made visible by lectin staining, optically-cleared tissue, and a deep tissue light-sheet microscopy (Fig. 2C∼E′). The images were stacked and reconstructed as a 3D structure of pancreatic tissue (Fig. 2F and Supplementary Data Video 3). Fully reconstructed 3D images are illustrated in Supplementary Data Video 4.

3. Vascular networks in islets

The number of arterioles entering into each islet depends upon the size of islets. The islets are randomly distributed across different lobes (Fig. 3A and Supplementary Data Video 5). Islets of various size are found in the pancreas because of the vast number and type of cells present within islets themselves (Fig. 3B). Corresponding histological slides are shown for comparison (Fig. 3C, D). In mice, most islets were found in an interlobular position (Fig. 3C′) rather than in an intralobular (Fig. 3C″). For better validation, lectin staining was performed in the pancreas sections where

www.kci.go.kr

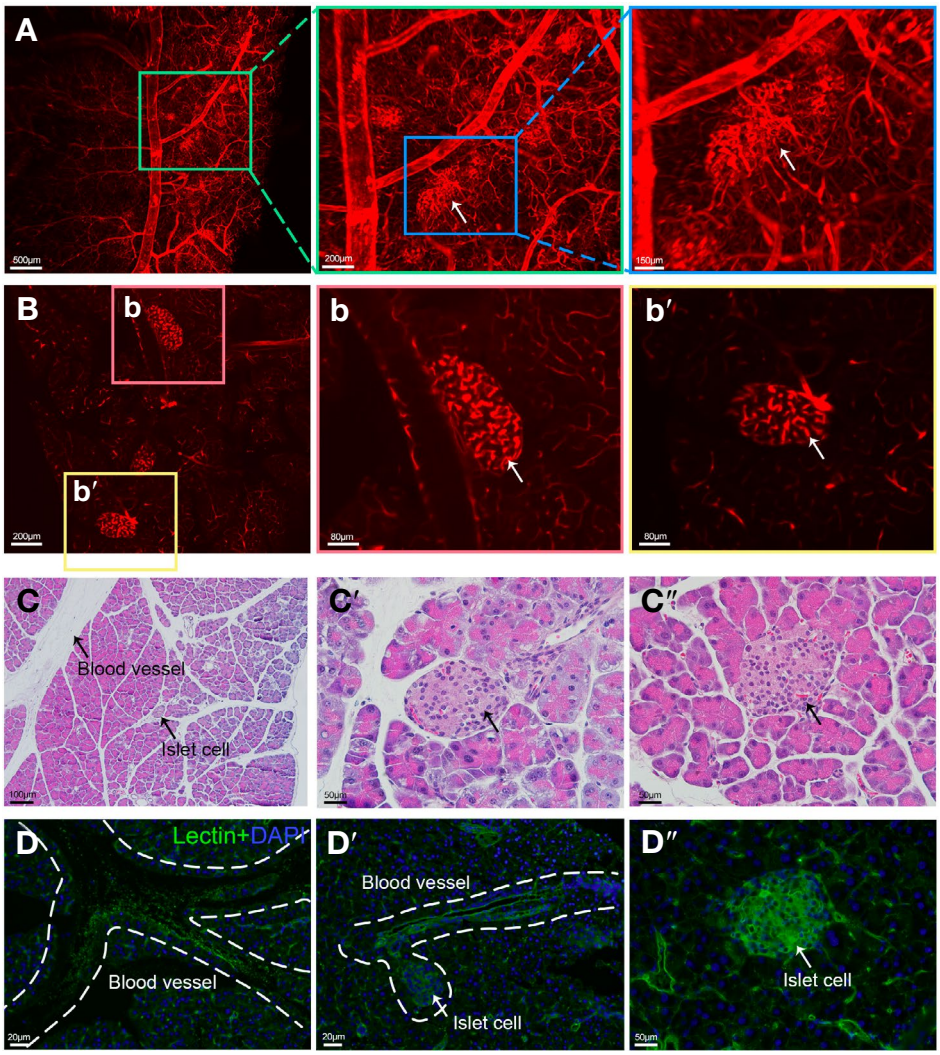

Fig. 3. Visualization of islet cells in a murine pancreas. (A): Islets are highly vascularized compartments of the pancreas, presented in the 3D images (white arrow). Enlarged figures are indicated in green and blue squares. (B): Different sizes and shapes of islet cells in the pancreas. (C∼D″): Histological slides shown for comparison with a 2D structure of islets and blood vessels in the pancreas. The blood vessel (C), interlobular (C′), and intralobular (C″) islets in tissue sections, stained with hematoxylin and eosin (H&E). (D∼D″): Lectin-stained tissue sections to show vascular system in the islets as well as in the pancreas. White dot line and arrow indicate blood vessel and islet cell. Scale: (A): 500 μm, 200 μm, 150 μm; (B): 200 μm, (b, b′): 80 μm; (C): 100 μm; (C′, C″): 50 μm; (D, D′): 20 μm; (D″): 50 μm.

stained islets were found (Fig. 3D″ and Supplementary Data Video 5). Blood vessels were labeled with lectin stains in 2D tissue sections (Fig. 3D, D′).

4. Quantifying and the size of islets

The number of β-cells affects the size and volume of islets and amount of insulin secretion, which is a key function of pancreas. So, the volume of islets was determined in this study. The total surface volume of vessels in pancreatic islets was quantified concurrently. To quantify the volume of islets in a whole pancreas, the lobular compartments were separated into three different parts based on the morphological features (Fig. 4A). Then, using the 3D isosurface calculation, the vessel network in each islet was created (Fig. 4B∼G). Islets were easily presented in yellow isosurface structure. The volume of each islet in gastric lobe, splenic lobe, and duodenal lobe were measured (Fig. 4H). Although the total number of islets in each lobe was different, the volume of islets in these lobes was not significantly different.

www.kci.go.kr

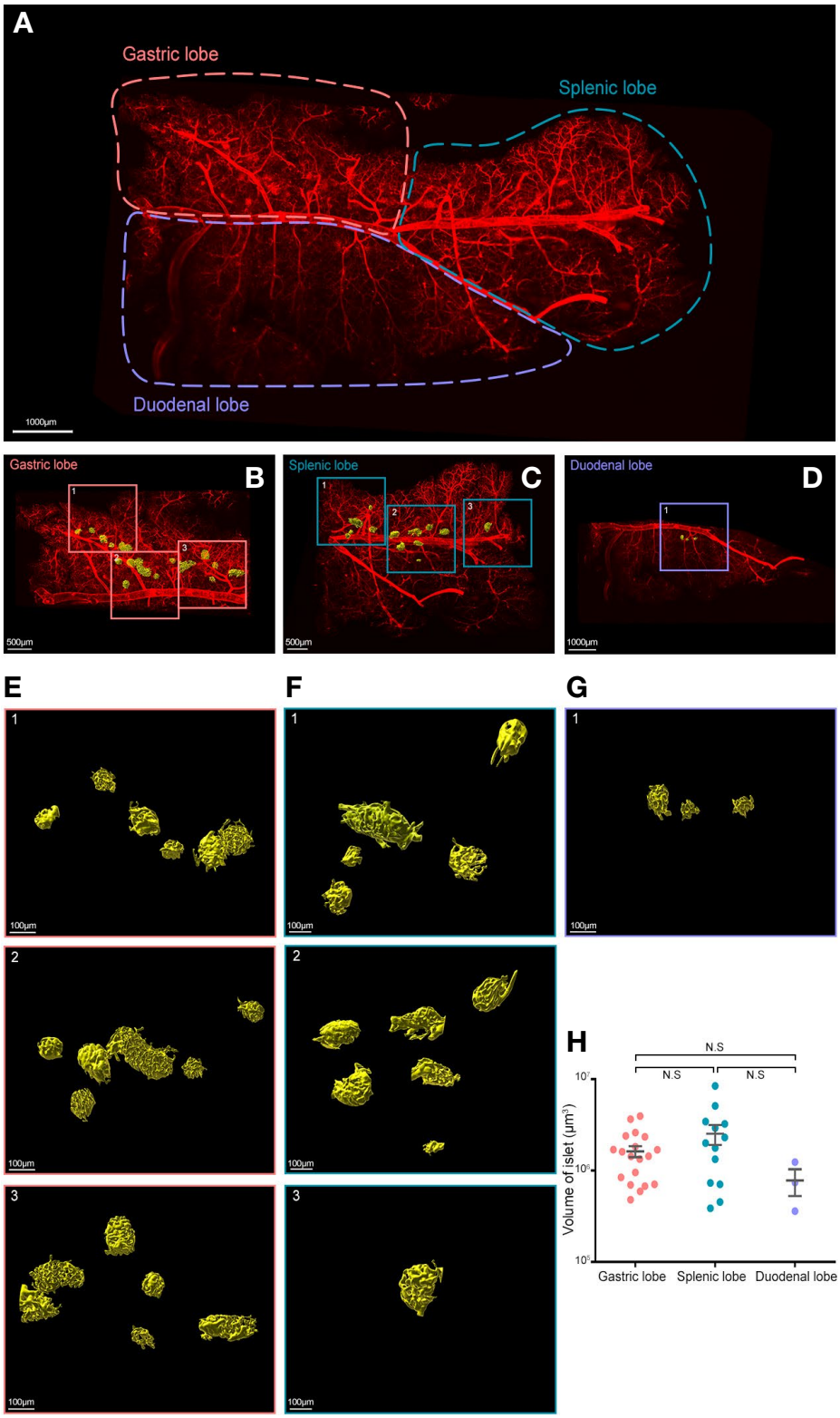

Fig. 4. Quantification of the size of islets. (A): 3D visualization of different parts of the murine pancreas. (B∼D): a pancreas tissue was separated into three lobes; (i) gastric lobe, (ii) splenic lobe, and (iii) duodenal lobe. (E∼G): Construction of isosurface structure of blood vessel in islet of three different lobes. The islets were magnified in subpanel of each lobes. (H) Quantification of each islet volume using isosurface calculation. The volume of islets was statistically analyzed using *t*-test for each anatomical lobe comparison and ANOVA for the group of every lobe to calculate p-value (significant if p-value < 0.05). Scale: (A): 1,000 μm; (B, C): 500 μm; (D): 1,000 μm; (E∼G): 100 μm.

DISCUSSION

Approximately 96%~99% of total pancreatic volume is comprised of exocrine pancreas, whereas only 1%~4% of its total volume is made up of endocrine structures [20,21]. To better understand generalized patterns of 3D vascular structures of the pancreas and islet cells under normal conditions, this study analyzed the murine pancreas by demonstrating a combined clearing and imaging approach. Many techniques have been developed to visualize vascular structures, which are often essential for detailed study, advanced diagnosis, and therapy [22-24]. Making opaque tissue transparent, thus allowing fluorescence imaging of blood vessels, facilitates visualization of their topology and 3D image reconstruction of organs. Recently various optical tissue clearing methods have been used for tissue clearing. Compared to other tissue clearing methods, our approach has the advantages in terms of tissue transparency and tissue conservation with relatively short tissue penetration time. In general, tissue clearing methods have harsh chemical processing such as organic solvent and detergent, leading to tissue damages. At the same time, the cleared tissue can be shrunken and distorted by removing the lipid membrane from the tissue clearing methods. In case of hydrogel-based methods, the longer incubation time and complex experimental methods can be issued though this method has several advantages such as uniform removal of lipids from the tissue with less damaging tissue [25]. Our clearing method retains endogenous protein fluorescence with immunostaining and provides the precise topological results without distortion and damaging its structure for 3D imaging.

Conventional confocal microscopy and two-photon microscopy are not practical for imaging large organs since they have a shallow depth of focus, require long acquisition times, and often result in photobleaching of samples. To overcome these limitations, LSFM was used as it is a versatile imaging technique that allows for rapid imaging of large volumes of cleared tissue with both high coverage and resolution [7,26,27]. In consistent, this study also emphasized LSFM technique for high depth and high-resolution imaging (Fig. 2F, 3D image). It is applicable for the imaging both individual tissue and entire organs at the same time with minimal photobleaching [28,29] and analyzing quantitative 3D segmentation of microvessel networks [30].

The 3D image reconstruction analysis is highly challenging since it requires considerable computational resources and many tools to analyze the large data sets produced. Imaris and custom software was used in this study for the reconstruction of pancreas vasculature structures as 3D images. As commercial software is highly advanced and rapidly evolving, their use is recommended for researchers who are unfamiliar with bioinformatics. Depending on the quality and quantity of images as well as available computational power, 1~2 days is required for 3D rendering, depending on the number, size, and resolution of the images. For higher image resolution, larger organ sizes, and greater number of images, more time is generally required to complete the rendering. In this study, total 246 shots of 2D images were used for 3D tissue rendering and analysis. Beside the reconstruction of 3D images of pancreas, this method is also applicable for the quantitative analysis of size of islets.

Even though the vascular structure of the pancreas can be reconstructed, there are certain limitations. One such limitation is that because lectin stains all blood vessel endothelial cells, veins are indistinguishable from arteries. To cater for this, two different lectin concentrations were used as well as variations in staining time; however, both attempts were unsuccessful. If a method is developed that successfully distinguishes between arteries and veins, it will be possible to investigate the topographical distribution of in-and-out vascular systems and their structures. This may require genetically-modified mice that are able to express fluorescent proteins only in targeted arteries and/or veins.

The tissue clearing technology is an important tool for the 3D imaging that allows topological deep tissue imaging in cellular and sub-cellular level. Since tissue sectioning is relatively not required, tissue clearing and 3D imaging can provide more reliable structural and functional information from biological specimen with less labor, enabling the quicker result and more accurate diagnosis of pathological disease. The impact of optical tissue clearing technique has been shown as a promising method to diagnosis of cardiovascular disease [31]. A current limitation of the tissue clearing technology is that it requires the high computational skill and power to reconstruct the 3D image, which is expected to be solved through a deep learning method.

In conclusion, high-resolution imaging of the vascular system of the pancreas and islets have been presented. The incorporation of lectin and optical tissue clearing with 3D rendering with Imaris provides an effective and suitable approach to visualize and quantify the vascular structure of

www.kci.go.kr

a pancreas. Hence, it can also provide more detailed topological information of vasculature system of an organ. In this way, this approach has a potential to advance various developmental biology field. These techniques with incorporation of immunostaining can be applicable to study the interconnection of various cells and blood vessels in disease development in human more precisely in future.

ACKNOWLEDGEMENTS

The authors wish to thank Binaree, Inc. for technical support and the Brain Research Core Facility, Korean Brain Research Institute, for image acquisition and rendering. This work was supported by the research grant of the Chungbuk National University Hospital in 2021 (Dr. Eu Jeong Ku). The funding source did not have any input in the study design, data collection, interpretation of the results, preparation of the manuscript, or publishing decision.

REFERENCES

1. Richardson DS, Lichtman JW. Clarifying Tissue Clearing. Cell. 2015;162:246-57.
2. Murray E, Cho JH, Goodwin D, Ku T, Swaney J, Kim SY, et al. Simple, Scalable Proteomic Imaging for High-Dimensional Profiling of Intact Systems. Cell. 2015;163:1500-14.
3. Dodt HU, Leischner U, Schierloh A, Jahrling N, Mauch CP, Deininger K, et al. Ultramicroscopy: three-dimensional visualization of neuronal networks in the whole mouse brain. Nat Methods. 2007;4:331-6.
4. Renier N, Wu Z, Simon DJ, Yang J, Ariel P, Tessier-Lavigne M. iDISCO: a simple, rapid method to immunolabel large tissue samples for volume imaging. Cell. 2014;159:896-910.
5. Hama H, Kurokawa H, Kawano H, Ando R, Shimogori T, Noda H, et al. Scale: a chemical approach for fluorescence imaging and reconstruction of transparent mouse brain. Nat Neurosci. 2011;14:1481-8.
6. Susaki EA, Ueda HR. Whole-body and Whole-Organ Clearing and Imaging Techniques with Single-Cell Resolution: Toward Organism-Level Systems Biology in Mammals. Cell Chem Biol. 2016;23:137-57.
7. Keller PJ, Dodt HU. Light sheet microscopy of living or cleared specimens. Curr Opin Neurobiol. 2012;22:138-43.
8. Kopylova VS, Boronovskiy SE, Nartsissov YR. Fundamental principles of vascular network topology. Biochem Soc Trans. 2017;45:839-44.
9. Ariel P. A beginner's guide to tissue clearing. Int J Biochem Cell Biol. 2017;84:35-9.
10. Yagihashi S. Diabetes and pancreas size, does it matter? J Diabetes Investig. 2017;8:413-5.
11. Yamazaki H, Tsuboya T, Katanuma A, Kodama Y, Tauchi S, Dohke M, et al. Lack of Independent Association Between Fatty Pancreas and Incidence of Type 2 Diabetes: 5-Year Japanese Cohort Study. Diabetes Care. 2016;39:1677-83.
12. Al-Mrabeh A, Hollingsworth KG, Steven S, Taylor R. Morphology of the pancreas in type 2 diabetes: effect of weight loss with or without normalisation of insulin secretory capacity. Diabetologia. 2016;59:1753-9.
13. Nishimura W, Sakaue-Sawano A, Takahashi S, Miyawaki A, Yasuda K, Noda Y. Optical clearing of the pancreas for visualization of mature beta-cells and vessels in mice. Islets. 2018;10:e1451282.
14. Love JA, Yi E, Smith TG. Autonomic pathways regulating pancreatic exocrine secretion. Auton Neurosci. 2007;133:19-34.
15. El-Gohary Y, Sims-Lucas S, Lath N, Tulachan S, Guo P, Xiao X, et al. Three-dimensional analysis of the islet vasculature. Anat Rec (Hoboken). 2012;295:1473-81.
16. Oh JW, Kloepper J, Langan EA, Kim Y, Yeo J, Kim MJ, et al. A Guide to Studying Human Hair Follicle Cycling In Vivo. J Invest Dermatol. 2016;136:34-44.
17. Wang Q, Oh JW, Lee HL, Dhar A, Peng T, Ramos R, et al. A multi-scale model for hair follicles reveals heterogeneous domains driving rapid spatiotemporal hair growth patterning. Elife. 2017;6:e22772.
18. Vanden Hoek TL, Goossens W, Knepper PA. Fluorescence-labeled lectins, glycoconjugates, and the development of the mouse AOP. Invest Ophthalmol Vis Sci. 1987;28:451-8.
19. Gautier MK, Ginsberg SD. A method for quantification of vesicular compartments within cells using 3D reconstructed confocal z-stacks: Comparison of ImageJ and Imaris to count early endosomes within basal forebrain cholinergic neurons. J Neurosci Methods. 2021;350:109038.
20. Saito K, Iwama N, Takahashi T. Morphometrical analysis on topographical difference in size distribution, number and volume of islets in the human pancreas. Tohoku J Exp Med. 1978;124:177-86.
21. In't Veld P, Marichal M. Microscopic anatomy of the human islet of Langerhans. Adv Exp Med Biol. 2010;654:1-19.
22. Preim B, Oeltze S,. 3D Visualization of Vasculature: An Overview2008; Berlin, Heidelberg: Springer Berlin Heidelberg.
23. Joshi A, Qian X, Dione DP, Bulsara KR, Breuer CK, Sinusas AJ, et al. Effective visualization of complex vascular structures using a non-parametric vessel detection method. IEEE Trans Vis Comput Graph. 2008;14:1603-10.

www.kci.go.kr

24. Liu P, Sun J, Zhao J, Liu X, Gu X, Li J, et al. Microvascular imaging using synchrotron radiation. J Synchrotron Radiat. 2010;17:517-21.
25. Ueda HR, Erturk A, Chung K, Gradinaru V, Chedotal A, Tomancak P, et al. Tissue clearing and its applications in neuroscience. Nat Rev Neurosci. 2020;21:61-79.
26. Hahn M, Nord C, Eriksson M, Morini F, Alanentalo T, Korsgren O, et al. 3D imaging of human organs with micrometer resolution - applied to the endocrine pancreas. Commun Biol. 2021;4:1063.
27. Lazzari G, Vinciguerra D, Balasso A, Nicolas V, Goudin N, Garfa-Traore M, et al. Light sheet fluorescence microscopy versus confocal microscopy: in quest of a suitable tool to assess drug and nanomedicine penetration into multicellular tumor spheroids. Eur J Pharm Biopharm. 2019;142:195-203.
28. Royer LA, Lemon WC, Chhetri RK, Wan Y, Coleman M, Myers EW, et al. Adaptive light-sheet microscopy for long-term, high-resolution imaging in living organisms. Nat Biotechnol. 2016;34:1267-78.
29. Reynaud EG, Krzic U, Greger K, Stelzer EH. Light sheet-based fluorescence microscopy: more dimensions, more photons, and less photodamage. HFSP J. 2008;2:266-75.
30. Kennel P, Teyssedre L, Colombelli J, Plouraboue F. Toward quantitative three-dimensional microvascular networks segmentation with multiview light-sheet fluorescence microscopy. J Biomed Opt. 2018;23:1-14.
31. Rioboo RJJ, Desco M, Gomez-Gaviro MV. Impact of optical tissue clearing on the Brillouin signal from biological tissue samples. Biomed Opt Express. 2019;10:2674-83.

SUPPLEMENTARY MATERIALS

The supplementary data videos for this article can be found online at:

Supplementary Data Video 1.
(https://doi.org/10.6084/m9.figshare.19492103.v1)
Supplementary Data Video 2.
(https://doi.org/10.6084/m9.figshare.19492118.v1)
Supplementary Data Video 3.
(https://doi.org/10.6084/m9.figshare.19492160.v1)
Supplementary Data Video 4.
(https://doi.org/10.6084/m9.figshare.19492163.v1)
Supplementary Data Video 5.
(https://doi.org/10.6084/m9.figshare.19492166.v1)

www.kci.go.kr